

of  $k_1$  cluster in an area centered about  $10^{-0.3}$  lower than the extrapolation. The statistical variation for the shock tube data prevents an accurate evaluation of  $E_1$  by themselves. However, an Arrhenius plot from the mean of the Flowers-Benson data to the mean of the shock tube data yields the equation:  $k_1 = 10^{13.2} \exp(-17.4 \text{ kcal}/RT)$ . These low values in  $k_1$  may reflect in part a somewhat lower temperature behind the reflected shock wave than is predicted by simple shock wave theory. Studies<sup>14,15</sup> of reflected shocks for argon in the region 1500–3000°K, considerably higher than in the present work, have indicated temperatures 30–60° lower than the predicted values. Still, standard deviation in  $\log k_1$  for the points amounts to 0.12 which will correspond to 0.8 kcal in the  $E_1$ . This  $E_1$  therefore lies within  $3\sigma$  of the value given by Flowers and Benson. They indicated that their value of  $E_1 = 20.0$  kcal gave a value for the bond dissociation energy of  $\text{CH}_3\text{I}$  about 1–2 kcal higher than other estimates, and the pre-exponential factor was somewhat high in view of the calculated collision number. Hence the present equation which makes use of the high-temperature data perhaps represents a better description of the kinetic behavior.

(14) R. A. Strehlow and A. Cohen, *J. Chem. Phys.*, **30**, 257 (1959).

(15) T. A. Brabbs, S. Z. Zlaterich, and F. E. Belles, *ibid.*, **33**, 307 (1960).

The mechanism involving the formation of methyl radicals appears quite ample to account for the exchange, and an alternative process such as the  $\text{SN}_2$  inversion proposed by Clark, *et al.*,<sup>4</sup> cannot play a major role. It does appear that even at their highest temperature they had not eliminated completely the effect of the wall catalysis.

The bimolecular decomposition of methyl iodide by argon was also tested as an alternative means for the methyl radical formation. With a preexponential factor of  $10^{14} \text{ sec}^{-1} \text{ cm}^3 \text{ mole}^{-1}$  as a limit for the expected collision frequency, an activation of only 35 kcal  $\text{mole}^{-1}$  would be required to provide even 10% of the reaction. Since this activation energy is 20 kcal below the bond dissociation energy, the contribution of this mechanism does not appear significant over the temperature range studied. Also, the bimolecular reaction of  $\text{I}_2$  with methyl iodide was eliminated since a collision frequency for a reasonable activation energy would be much in excess of theoretical values.

The experimental data appear therefore to be consistent with a mechanism involving the formation of a methyl radical in the collision between an iodine atom and methyl iodide which now has been rather well established for several recent kinetics studies.<sup>5,6,13,16</sup>

(16) C. A. Goy, A. Lord, and H. O. Pritchard, *J. Phys. Chem.*, **71**, 1086 (1967).

## The Rate of Bridge-Terminal Proton Exchange in $\mu$ -Dimethylamino-diborane

Roger E. Schirmer, Joseph H. Noggle, and Donald F. Gaines

Contribution from the Department of Chemistry, University of Wisconsin, Madison, Wisconsin 53706. Received June 2, 1969

**Abstract:** The intramolecular hydrogen exchange in  $\mu$ -dimethylamino-diborane has been studied by fitting the line shape of the  $^{11}\text{B}$  nmr spectrum as a function of temperature. Relaxation matrix theory was used to establish a model for the line shape, and it was found necessary to consider the temperature dependence of both the exchange rate constant and the line-width parameter in order to reproduce the observed spectra over the full temperature range studied (213–373°K). A nonlinear least-squares program was used to extract values of these parameters from the spectra. The boron-bridge hydrogen and the boron-terminal hydrogen coupling constants were found to be 33.0 and 129.3 Hz, respectively. They are of the same sign and temperature independent. The exchange process was studied in solution in 1,2-dimethoxyethane, tetrahydrofuran (four concentrations), methylcyclohexane (two concentrations), and the neat liquid. The rate constant is found to have two components and may be written  $k(T, C) = k_1(T) + Ck_2(T)$ , where  $k_1$  is the rate constant in inert solvents and in the neat material,  $k_2$  is the rate constant for the ether-catalyzed exchange process, and  $C$  is the concentration of the ether. The results obtained were  $\Delta S^\ddagger = 0.4 \pm 0.3 \text{ cal/deg}$  and  $\Delta H^\ddagger = 16.9 \pm 0.1 \text{ kcal/(deg mole)}$  in methylcyclohexane and the neat liquid,  $\Delta S^\ddagger = -25.5 \pm 0.1 \text{ cal/deg}$  and  $\Delta H^\ddagger = 6.1 \pm 0.4 \text{ kcal/(deg mole)}$  for the catalyzed process in tetrahydrofuran, and  $\Delta S^\ddagger = -28.7 \pm 0.4 \text{ cal/deg}$  and  $\Delta H^\ddagger = 6 \pm 1 \text{ kcal/(deg mole)}$  in 1,2-dimethoxyethane. The ranges are standard errors.

The  $^{11}\text{B}$  nmr spectrum of  $\mu$ -dimethylamino-diborane is strongly temperature dependent due to intramolecular exchange of the bridge and terminal hydrogens (see Figure 1).<sup>1,2</sup> Gaines and Schaeffer<sup>2</sup> reported the rate of exchange in ether solutions to increase with

(1) W. D. Phillips, H. C. Miller, and E. L. Muetterties, *J. Am. Chem. Soc.*, **81**, 4496 (1959).

(2) D. F. Gaines and R. Schaeffer, *ibid.*, **86**, 1505 (1964).

increasing base strength of the ether, and they estimated an activation energy of 3.7 kcal/mole for the process in 1,2-dimethoxyethane. They also discuss the mechanism of this exchange and conclude that it probably proceeds by cleavage of a boron-bridge hydrogen bond followed by rotation of the  $-\text{BH}_3$  group and reestablishment of the bridge bond. If this mechanism is correct, the observed acceleration of exchange by Lewis bases

would be due to reversible nucleophilic attack of the base on the boron, thus facilitating the bridge-opening step.

We have obtained rates and activation energies for this exchange process in the neat liquid and in solutions in methylcyclohexane, 1,2-dimethoxyethane, and tetrahydrofuran. The procedure was to establish a model for the line shape using Redfield's<sup>3</sup> relaxation matrix formalism as a guide. While neglect of all off-diagonal elements of the relaxation matrix other than the exchange elements reduces these equations to a set of exchange-coupled Bloch equations, the terminology of Redfield's theory has been kept to facilitate discussion of the assumptions involved in this treatment. Characteristic values of the parameters appearing in these equations were determined by least-squares fits of the equations to several of the experimental spectra. These values were then used to compute a series of spectra covering a wide range of exchange rates, and rates of exchange for the remaining experimental spectra were obtained by comparison with these calculated spectra. The results of these comparisons were checked by a least-squares analysis on spectra at two or three temperatures for each sample. The excessive cost of the least-squares procedure, which required about 5 min per iteration on a CDC 1604 computer, prohibited using it for all the data points.

### Theory

**Line-Shape Equations.** The Hamiltonian for the spin system may be written as a sum of three parts

$$H(t) = H^0 + E(t) + H'(t) \quad (1)$$

where  $H^0$  includes the Zeeman effect and spin-spin coupling and is time independent,  $E(t)$  is the coherent perturbation of the applied radiofrequency field, and  $H'(t)$  is the random perturbation which causes relaxation.  $H'(t)$  can be written as the sum of operator products<sup>4</sup>

$$H'(t) = \sum_q F^q(t) A^q \quad (2)$$

where the  $F^q$ 's are stationary random functions of the lattice variables and the  $A^q$ 's are operators on the spin variables. Chemical exchange operators may be included in the  $A^q$ .<sup>5</sup> Redfield's<sup>3</sup> approximate equation of motion for the spin density matrix is then

$$d\sigma/dt = -i[H^0 + E(t), \sigma] - \Gamma(\sigma - \sigma^0) \quad (3)$$

where

$$\Gamma_{kl}(\sigma - \sigma^0) = -\sum_{mn} R_{klmn}(\sigma_{mn} - \sigma_{mn}^0)$$

While the development of eq 3 assumes extreme narrowing for all the relaxation processes, we shall assume, along with Alexander<sup>6</sup> and Gutowsky, Vold, and Wells,<sup>7</sup> that the equation is valid for all rates of exchange. Written in the basis of eigenfunctions of  $H^0$ , eq 3 becomes

$$dz_{kl}/dt = i(\omega - \omega_{kl})z_{kl} + id_{kl}(\sigma_{kk} - \sigma_{ll}) - \Gamma_{kl}(z) \quad (4)$$

(3) A. G. Redfield, *IBM J. Res. Develop.*, **1**, 19 (1957); also in *Advan. Magnetic Resonance*, **1**, 1 (1965).

(4) A. Abragam, "Principles of Nuclear Magnetism," Oxford University Press, London, 1961, Chapter 8.

(5) J. Kaplan, *J. Chem. Phys.*, **28**, 278 (1958); **29**, 462 (1958).

(6) S. Alexander, *ibid.*, **37**, 967 (1962).

(7) H. S. Gutowsky, R. L. Vold, and E. J. Wells, *ibid.*, **43**, 4107 (1965).

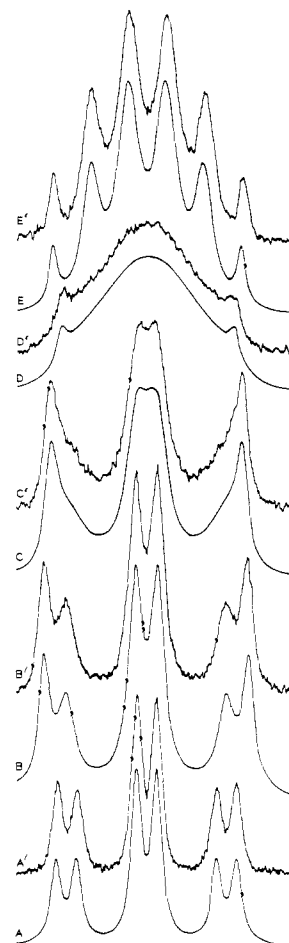


Figure 1. Comparison of experimental (primed labels) with calculated  $^{11}\text{B}$  nmr spectra of  $\mu\text{-(CH}_3)_2\text{NB}_2\text{H}_5$ . A and D are spectra of the neat sample at 10 and 80°, respectively. B, C, and E are spectra of the 50 mole % sample in methylcyclohexane at 35, 49, and 104°, respectively. The sequence from A to E shows the typical dependence of this spectrum on increasing temperature. Table I contains the numerical data obtained from these spectra.

where

$$z_{kl} = e^{i\omega t} \sigma_{kl}, \quad d_{kl} = 1/2 \sum_s \gamma_s H_1(k|I_+(s)|l)$$

and

$$\Gamma_{kl} = -\sum_{mn} R_{klmn} z_{mn} \quad (k \neq l, m \neq n)$$

and where  $\omega$  is the frequency of  $E(t)$ ,  $H_1$  is its intensity, and the index  $s$  runs over all spins.

To obtain the slow-passage line shape, the derivatives in eq 4 are set equal to zero. The quantities  $\sigma_{kk}$  appearing in eq 4 are the populations of the spin states. In the absence of saturation they may be approximated by their equilibrium values, and then using the high-temperature approximation

$$id_{ij}(\sigma_{ii} - \sigma_{jj}) \approx id_{ij}(\sigma_{ii}^0 - \sigma_{jj}^0) \approx id_{ij} \hbar \omega_{ij} / kT \equiv a_{ij}$$

Making these substitutions in eq 4 and collapsing the indices by  $kl \rightarrow A$  and  $mn \rightarrow B$  we obtain

$$i\omega z_A - i\omega_A z_A + \sum_B R_{AB} z_B = -ia_A \quad (5)$$

The slow-passage line shape is given by

$$I(\omega) = \sum_{kl} \text{Im} \langle l|I_+|k \rangle z_k e^{i\omega t} = c \sum_A \text{Im} z_A \quad (6)$$

The last form of this equation depends upon the elements of  $I_+$  being the same for each term in the sum. This will always be true for spins  $1/2$ , and is true in the case dealt with here when the  $z_A$ 's refer to the quantities in the reduced problem (see Appendix II). To solve eq 5 for  $I(\omega)$  they are first put into matrix form using the following definitions:  $\mathbf{R} = [R_{AB}]$ ,  $\mathbf{\Omega} = [\omega_A \delta_{AB}]$ ,  $\mathbf{S} = -\mathbf{\Omega} - i\mathbf{R}$ ,  $\mathbf{z} = [z_A]$ , and  $\mathbf{a} = [a_A]$ . Equations 5 can then be written as the single matrix equation

$$i\omega\mathbf{z} - i\mathbf{\Omega}\mathbf{z} + \mathbf{R}\mathbf{z} = -i\mathbf{a}$$

which rearranges to

$$(\mathbf{S} - \mathbf{I}\omega)\mathbf{z} = -\mathbf{a} \quad (7)$$

where  $\mathbf{I}$  is the identity matrix. Equation 7 is in a convenient form for computerized calculation of the line shape. Details of the solution, which requires determining the eigenvalues and eigenvectors of the complex matrix  $\mathbf{S}$ , are given in Appendix I.

**The R Matrix.** Examination of both the boron and hydrogen nmr of  $\mu$ -dimethylamino-diborane shows that each boron is coupled to one bridge and two terminal hydrogens. There is no indication of boron-boron or other long-range  $J$  couplings such as have been reported for diborane.<sup>8</sup> However, each boron is coupled to the distant hydrogens by exchange. This can be seen from the high-temperature  $^{11}\text{B}$  spectrum which is a sextet indicating that all five hydrogens are equivalent on the nmr time scale. While the equivalence of the borons allows us to compute the  $^{11}\text{B}$  nmr line shape by considering transitions of only one boron, all five hydrogens must be included.

The spin product functions for this system may be written  $\Psi\phi_1\phi_2|\phi_3|\phi_4\phi_5$ , where  $\Psi$  is the boron spin state,  $\phi_1$  and  $\phi_2$  are the spin states of the terminal hydrogens bonded directly to this boron,  $\phi_3$  is the state of the bridge hydrogen, and  $\phi_4$  and  $\phi_5$  are the states of the distant terminal hydrogens. There are 128 such spin product functions and a correspondingly large number of allowed boron transitions. However, as shown in Appendix II, the dimension of this problem can be greatly reduced if it is assumed that only quadrupole relaxation is important for the boron nucleus. Applying this assumption reduces the relaxation matrix to a  $32 \times 32$  matrix, the rows and columns of which are conveniently labeled by the hydrogen part of the spin product functions.

The transitions observed experimentally may be written  $\Psi\phi \rightarrow \Psi'\phi$ ; *i.e.*, they connect states which differ only in the boron part of the spin product function and not in the hydrogen part. In the absence of boron-hydrogen cross relaxation, the relaxation operators will be either pure boron or pure hydrogen spin operators and will induce transitions of the types  $\Psi\phi \rightarrow \Psi'\phi$  or  $\Psi\phi \rightarrow \Psi\phi'$ , respectively. Thus, the off-diagonal element  $R_{AB}$  of the relaxation matrix will connect transitions  $\Psi_a\phi_A \rightarrow \Psi_b\phi_A$  with transitions  $\Psi_a\phi_B \rightarrow \Psi_b\phi_B$ . The elements of the relaxation matrix are given by<sup>3</sup>

$$R_{klmn} = J_{kmln} - \frac{1}{2}\delta_{ln}\sum_r J_{krmr} - \frac{1}{2}\delta_{km}\sum_r J_{lrrn} \quad (8)$$

where

$$J_{kmln} = \sum_q J^q \langle k|A^q|m\rangle \langle l|A^q|n\rangle^* \quad (9)$$

(8) T. C. Farrar, R. B. Johannsen, and T. D. Coyle, *J. Chem. Phys.*, **49**, 281 (1968).

The  $A^q$ 's are the spin operators of eq 2, and  $\delta$  is the Dirac delta function. If the indices  $klmn$  are associated with spin states according to

$$k = \Psi_a\phi_A, l = \Psi_b\phi_A, m = \Psi_a\phi_B, \text{ and } n = \Psi_b\phi_B,$$

then the off-diagonal elements  $R_{klmn}$  may be written explicitly as

$$\begin{aligned} R_{klmn} &= \sum_q J^q \langle \Psi_a\phi_A | A^q | \Psi_a\phi_B \rangle \langle \Psi_b\phi_A | A^q | \Psi_b\phi_B \rangle^* \\ &= \sum_q J^q \langle \Psi_a | \Psi_a \rangle \langle \phi_A | A^q | \phi_B \rangle \langle \Psi_b | \Psi_b \rangle^* \langle \phi_A | A^q | \phi_B \rangle^* \\ &= \sum_q J^q |\langle \phi_A | A^q | \phi_B \rangle|^2 \equiv R_{AB} \end{aligned} \quad (10)$$

$$k \neq l, m \neq n, k \neq m$$

Since the  $^{11}\text{B}$  transitions will correspond uniquely to the proton spin functions,  $A$  and  $B$  can and do refer to both. The prime on the sum indicates it is taken over hydrogen spin operators only. The terms corresponding to boron spin operators are all zero as they all contain the factor  $\langle \phi_A | \phi_B \rangle$  which is zero by the orthogonality of the hydrogen spin product functions. The  $R_{AB}$  in eq 10 indicates the position of the element  $R_{klmn}$  in the collapsed  $R$  matrix.

If the preceding analysis is carried through for a diagonal element,  $R_{mnmn}$ , the result is

$$R_{mnmn} = R_{mnmn}(B) - \sum_{\tau \neq B} \sum_q J^q |\langle \phi_B | A^q | \phi_\tau \rangle|^2 \quad (11)$$

where the first term contains only the contributions from boron operators and the second from only the hydrogen operators. Comparing eq 10

$$R_{mnmn} = R_{mnmn}(B) - \sum_{\tau \neq B} R_{B\tau}$$

or

$$R_{BB} = R_B^0 - \sum_{\tau \neq B} R_{B\tau} \quad (12)$$

where  $R_B^0 = R_{mnmn}(B)$  and is independent of exchange. Thus the diagonal elements may be written as an exchange-independent term,  $R_B^0$ , minus the sum of the off-diagonal elements of the  $B$ th row. For a single boron nucleus in the absence of interaction with other spins,  $R_B^0$  would reduce to  $(T_{2B})^{-1}$ , the reciprocal of the spin-spin relaxation time of an uncoupled  $^{11}\text{B}$  nucleus and the  $^{11}\text{B}$  line width in the absence of exchange. In the calculations reported here, a single value,  $R(T)$ , was assumed for all the  $R_B^0$ . This assumption is rigorous if boron relaxation is dominated by quadrupole relaxation (see Appendix II). Preliminary calculations showed that the temperature dependence of the line width was essential to reproduce the temperature dependence of the spectrum over the whole range studied (about 213–383 °K).

The exchange mechanism we have assumed involves interchange of a bridge and a terminal hydrogen. Because of this, the exchange rate constant,  $k(T)$ , appears in the relaxation matrix at positions connecting hydrogen spin functions which differ only by the interchange of the spin state of the bridge hydrogen and one of the four terminal hydrogens. Equation 12 shows that, for every  $k$  appearing in one of these off-diagonal positions, a  $-k$  is added to the corresponding diagonal element. For example,  $k$  would appear in the matrix elements connecting the function  $\alpha\alpha|\beta|\alpha\beta$  with  $\alpha\alpha|\alpha|\beta\beta$ , and  $-k$  would appear in the corresponding diagonal element.

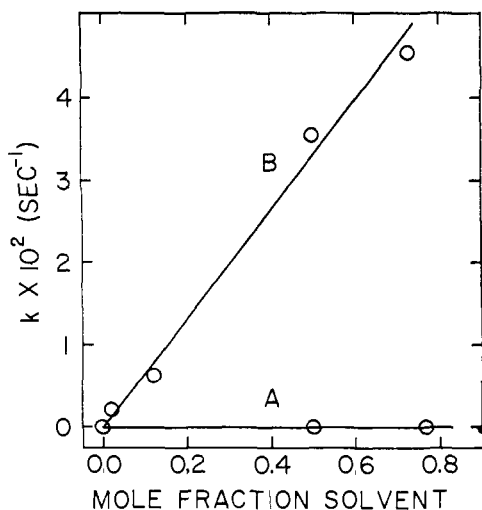


Figure 2. The rate constant  $k$  at  $10^\circ$  as a function of the mole fraction of solvent: (A) in methylcyclohexane, (B) in tetrahydrofuran. Points plotted represent least-squares smoothed data in order to represent the rate at a single temperature.

Two additional parameters,  $Q_1$  and  $Q_2$ , were included as off-diagonal elements in the  $R$  matrix in several calculations.  $Q_1$  connected boron transitions whose hydrogen spin functions differed by inversion of only one spin, and  $Q_2$  connected transitions whose hydrogen spin functions differed by inversion of two spatially adjacent spins (terminal-terminal on the same boron or bridge-terminal). Both of these types of elements could be caused by proton dipole-dipole relaxation and are expected to be on the order of  $T_{1H}^{-1}$ . These calculations were intended to determine whether or not nonsecular elements neglected in setting up the relaxation matrix might be important in determining the line shape. Values of the four parameters,  $Q_1$ ,  $Q_2$ ,  $k$ , and  $R$ , were determined by a least-squares fit of the equations to several low-temperature spectra. Low-temperature spectra were used because the large values of  $k(T)$  found at higher temperatures would mask other small contributions to the line shape. In several cases spectra were computed for a range of values of  $Q_1$  and  $Q_2$  around the least-squares value, but keeping  $k$  and  $R$  fixed. In all cases the values of  $Q_1$  and  $Q_2$  obtained were small compared to  $R$  and  $k$ , and their effects on the line shape were entirely negligible. These and other nonsecular relaxation elements were ignored in subsequent calculations.

After writing out the  $32 \times 32$  matrix, it was found that several of the remaining coincident transitions could also be collapsed (even in cases where  $Q_1$  and  $Q_2$  were included). This resulted in an  $18 \times 18$  (unsymmetric) matrix which was used in the calculations.

### Experimental Section

$\mu$ -Dimethylamino-diborane was prepared by the method of Burg and Randolph<sup>9</sup> using standard high-vacuum techniques. Its purity was checked by comparing vapor pressures<sup>9</sup> and infrared spectra<sup>10</sup> with those published previously.

The nmr samples were prepared on the vacuum line. The  $\mu$ -dimethylamino-diborane and carefully dried solvents were measured as gases and condensed into 5-mm nmr tubes, which were then sealed and stored at  $-78^\circ$  until used.

(9) A. B. Burg and C. L. Randolph, *J. Am. Chem. Soc.*, **71**, 3451 (1949).

(10) D. E. Mann, *J. Chem. Phys.*, **22**, 70 (1954).

Spectra were obtained using a Varian HA-100 spectrometer equipped with a V-4311 32.1-Mc fixed-frequency unit and corresponding probe, and a V-4343 temperature controller. As there was some problem with instability in the temperature controller, temperatures were measured with a copper-constantan thermocouple in an nmr tube of either toluene or glycerine. This tube was inserted in the probe and the temperature measured both before and after each spectrum was recorded. The temperatures are accurate to  $\pm 1^\circ$ . The standard side-band technique was used to calibrate the spectra.

Field homogeneity was adjusted by maximizing the resolution in a neat sample of the  $\mu$ -dimethylamino-diborane. Examination of the  $^{11}\text{B}$  spectrum of the  $\text{BF}_4^-$  (coupling constant 1.5 Hz) after adjusting the homogeneity in this way indicated a resolution of at least 1 Hz. Care was taken in all cases to avoid saturation, over-filtering, too rapid a sweep, or drift, any of which could distort the line shape.

### Calculations and Results

If all frequencies are expressed in radians/second, the rate constant  $k$  is the frequency of exchange in reciprocal seconds. To obtain its temperature and concentration dependence (in basic solvents), it was necessary to assume that exchange occurs by two different mechanisms. The first mechanism, which is responsible for the exchange observed in the absence of Lewis base, is concentration independent as can be seen from line A of Figure 2. The second mechanism represents the base-catalyzed exchange process which line B of Figure 2 shows to be first order in the base. The temperature dependence of these rate constants is described very well by the equation<sup>11</sup>

$$k = (kT/h) \exp\left(\frac{\Delta S^\ddagger}{R} - \frac{\Delta H^\ddagger}{RT}\right) \quad (13)$$

where  $k$  is Boltzmann's constant,  $h$  Planck's constant,  $\Delta S^\ddagger$  the entropy of activation, and  $\Delta H^\ddagger$  the enthalpy of activation. The over-all rate constant  $k$  observed in the presence of base may thus be written

$$k = k_1 + k_2 = (kT/h) \exp\left(\frac{\Delta S_1^\ddagger}{R} - \frac{\Delta H_1^\ddagger}{RT}\right) + ([B]kT/h) \exp\left(\frac{\Delta S_2^\ddagger}{R} - \frac{\Delta H_2^\ddagger}{RT}\right) \quad (14)$$

where  $[B]$  is the base concentration.

In methylcyclohexane solution exchange proceeds entirely by the first mechanism, thus allowing the constants  $\Delta S_1^\ddagger$  and  $\Delta H_1^\ddagger$  to be evaluated. Substituting these values into eq 14, along with experimental  $k$ 's, then allows evaluation of the corresponding constants for the catalyzed reaction.

Initial calculations were done on the neat sample. In these preliminary calculations the coupling constants  $J_B$  (boron-bridge hydrogen) and  $J_T$  (boron-terminal hydrogen) were varied as well as  $R$ ,  $k$ , and in a few cases  $Q_1$  and  $Q_2$ . The results were  $J_B = 33.0$  Hz and  $J_T = 129.3$  Hz as compared with values of 30 and 130 previously reported.<sup>2</sup> The values 33.0 and 129.3 were used in all subsequent calculations. There was no indication of temperature or solvent dependence in these coupling constants,<sup>12</sup> even though changes on the order of 0.5 Hz should have been detectable.

With the  $J$ 's fixed, spectra corresponding to two or three temperatures for each sample were fit. Input to

(11) W. F. K. Wynne-Jones, and H. Eyring, *ibid.*, **3**, 492 (1935).

(12) P. Laszlo in "Progress in Nuclear Magnetic Resonance Spectroscopy," Vol. 3, J. W. Emsley, J. Feeney, and L. H. Sutcliffe, Ed., Pergamon Press, New York, N. Y., 1967, p 231.

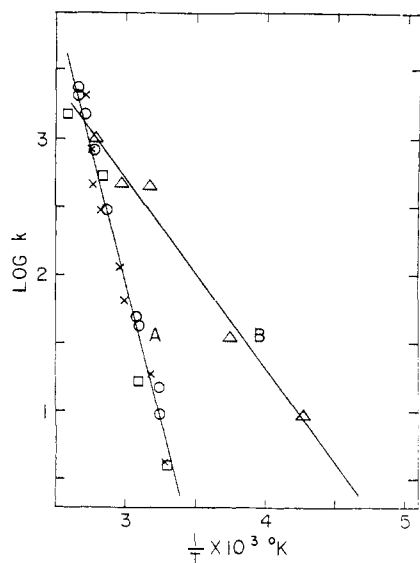


Figure 3. (A) Rate constants ( $k_1$ ) for the uncatalyzed process obtained for the neat sample ( $\square$ ), for 50 mole % in methylcyclohexane ( $\circ$ ), and for 23 mole % in methylcyclohexane ( $\times$ ). (B) Rate constants ( $k_2$ ) for the catalyzed exchange process in a 50 mole % sample in 1,2-dimethoxyethane ( $\Delta$ ).

the computer consisted of frequencies and amplitudes at 17 to 38 points from one-half of the spectrum. The results of these calculations, along with mean-square deviations and amplitude maxima, are collected in Table I.

Table I. Rate Constants and Line Widths for Spectra Fit by Computer

Solvent (mole fraction of $\mu$ - $(\text{CH}_3)_2\text{NB}_2\text{H}_3$ )	Temp, $^\circ\text{C}$	$k$ , $\text{sec}^{-1}$	$R$ , $\text{sec}^{-1}$	Rms dev, in.	Max spectral amplitude, in.
Neat	80	509.6	58.4	0.03	4.89
	49	16.3	52.2	0.03	4.33
	30	3.8	50.3	0.03	5.71
	10	0.1	48.4	0.06	6.35
Methylcyclohexane (0.50)	104	2216.6	37.1	0.06	8.31
	49	47.8	37.7	0.06	6.84
	35	14.5	38.3	0.03	8.15
Tetrahydrofuran (0.98)	48	91.7	49.0	0.03	6.20
	9	6.3	55.3	0.05	7.66
Tetrahydrofuran (0.88)	30	153.3	33.3	0.03	6.38
	9	57.8	41.5	0.06	7.05
	-52	3.1	79.2	0.05	6.77
Tetrahydrofuran (0.50)	60	3024.6	29.5	0.04	6.59
	10	289.0	43.9	0.07	7.72
	-50	9.4	79.2	0.02	7.37
Tetrahydrofuran (0.27)	50	2743.8	57.2	0.02	4.71
	10	493.2	53.4	0.2	4.17
	-42	31.4	79.2	0.04	5.70

The quality of the fits obtained is apparent from Figure 1 where several pairs of experimental and calculated spectra are reproduced.

The remaining values of  $k$  were obtained by comparison of the experimental spectra with a series of calculated spectra for which the  $k$ 's were known. The standard spectra were computed at  $10^\circ$  intervals from 213

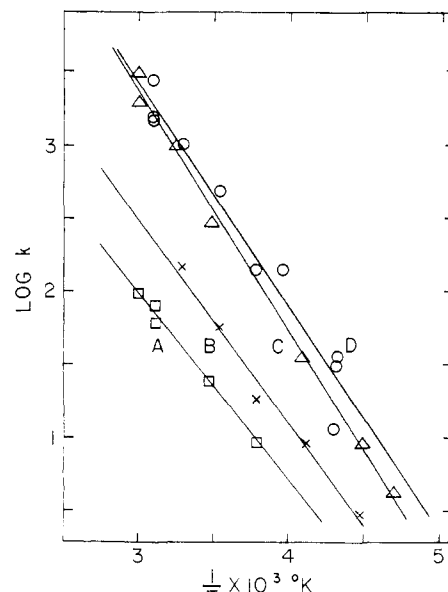


Figure 4. Rate constants ( $k_2$ ) for the catalyzed exchange process in several solutions of different concentrations in tetrahydrofuran. The mole per cent  $\mu$ - $(\text{CH}_3)_2\text{NB}_2\text{H}_3$  in these is (A) 98%,  $\square$ ; (B) 88%,  $\times$ ; (C) 50%,  $\Delta$ ; (D) 27%,  $\circ$ .

to  $333^\circ\text{K}$  using the values of  $R$  and  $k$  given by

$$R(T) = 4.98 \exp(1.23 \times 10^3/RT)$$

$$k_1(T) = 1.09 \times 10^8 \exp(-7.23 \times 10^3/RT) \quad (15)$$

These relations were obtained by fitting simple exponentials to the data given in Table I for the 50 mole % sample in tetrahydrofuran, it being assumed that this procedure would provide suitably typical temperature dependence for the purpose of comparison. The units are radians per second for the preexponential factors and calories/mole in the exponent. The  $R$  in the exponent is, as usual, the gas constant. It should be noted that the "activation energy" of 1.23 kcal/mole obtained for  $R$  is in the range normally found for line widths in solvents which do not hydrogen bond.<sup>13</sup>

The rate data obtained by both least-squares calculation and by comparison are presented in Figures 3 and 4. All values obtained in the absence of catalyst fall on curve A of Figure 3. The remaining curves represent only the rate constants for the catalyzed exchange. The uncatalyzed contributions in these cases were calculated from the combined data on the two methylcyclohexane solutions and then subtracted from the observed constant. In calculating the entropies of activation, the concentration appearing in eq 14 was expressed as mole fraction. The entropies and enthalpies of activation for each sample are collected in Table II.

## Discussion

The mechanism of exchange considered here would imply a small positive entropy of activation in the uncatalyzed reaction as bridge opening would transfer a vibrational mode to a rotational one, and perhaps result in lowering the energy of other vibrational modes as well. The mean value of  $\Delta S_1^\ddagger = 0.4 \pm 0.3$  cal/deg is in good agreement with this.

(13) H. G. Hertz in ref 12, p 198.

Table II. Enthalpies and Entropies of Activation

Solvent	Mole fraction of $\mu$ - (CH <sub>3</sub> ) <sub>2</sub> - NB <sub>2</sub> H <sub>5</sub>	$\Delta H^\ddagger$ , kcal/mole	$\Delta S^\ddagger$ , cal/deg
Neat	1.00	17.1 $\pm$ 0.4	1 $\pm$ 1
Methylcyclohexane	0.50	16.8 $\pm$ 0.1	0.8 $\pm$ 0.4
	0.23	16.7 $\pm$ 0.3	-0.1 $\pm$ 0.7
	0.98	5.22 $\pm$ 0.07	-27.5 $\pm$ 0.3
Tetrahydrofuran	0.88	5.90 $\pm$ 0.09	-26.5 $\pm$ 0.3
	0.50	6.91 $\pm$ 0.04	-22.3 $\pm$ 0.2
	0.27	6.30 $\pm$ 0.09	-25.8 $\pm$ 0.3
	1,2-Dimethoxyethane	0.50	6 $\pm$ 1

The large negative entropy of activation ( $-25.5 \pm 0.1$  and  $-28.7 \pm 0.4$  cal/deg in tetrahydrofuran and 1,2-dimethoxyethane, respectively) found for the catalyzed process reflects the formation of a specific reactant-catalyst complex, although in all probability a very short-lived one, with a resulting decrease in the available degrees of freedom. The approximate equality of the  $\Delta S_2^\ddagger$  values in all concentrations in tetrahydrofuran and in 1,2-dimethoxyethane shows that changes in solution structure about the  $\mu$ -dimethylamino-diborane do not contribute significantly to  $\Delta S_2^\ddagger$ .

Comparison of the values of  $k$  at a given temperature in tetrahydrofuran and 1,2-dimethoxyethane shows the dependence of this quantity on the base strength of the ether as reported previously by Gaines and Schaeffer.<sup>2</sup> The values of  $\Delta S_2^\ddagger$  and  $\Delta H_2^\ddagger$  do not reflect this difference unless it is considered significant that the  $\Delta S_2^\ddagger$  term for the 1,2-dimethoxyethane is higher than any obtained in tetrahydrofuran. It would not be surprising to find very similar  $\Delta H_2^\ddagger$  values for most ethers, with the main difference between them being in the entropy term. However, the scatter in our data is too great to confirm this even for the two ethers studied here.

Gaines and Schaeffer<sup>2</sup> also noted that the outermost peaks in the spectrum were present at all temperatures and that the spacing between them was constant. From our model it can be seen that these peaks are due to transitions between boron states with the hydrogen spin functions  $\alpha\alpha|\alpha|\alpha\alpha$  and  $\beta\beta|\beta|\beta\beta$  which cannot be coupled to any other hydrogen functions by exchange and thus remain relatively unaffected by temperature changes. This, in turn, shows that  $J_T$  and  $J_B$  have the same relative sign, as otherwise the boron transitions corresponding to these hydrogen spin states would not be the outermost lines of the spectrum.

A small but consistent deviation of the computed from the experimental spectra should also be mentioned. In the computed spectra the amplitudes in the tails and in the valleys are consistently somewhat greater than in the experimental spectra. As the calculations provide the best fit (using the least-squares criterion for goodness of fit) of the model to the experiment, this deviation must be attributed to shortcomings of the model itself. For example, the use of a single width,  $R(T)$ , for all lines could produce this sort of deviation if the lines did, in fact, have significantly different widths. The presence of small unresolved  $J$  couplings could also alter the line shape in the observed manner as could magnetic field inhomogeneities and detector filtering. Whatever the source of this discrepancy, the effect is too small to be of significance in the study reported here.

**Acknowledgment.** This research was supported by the Petroleum Research Fund under Grant No. 3015-A3, whose support is gratefully acknowledged. Computations were performed using the facilities of the University of Wisconsin Computing Center. Nmr spectra were obtained using the University of Wisconsin Chemistry Department Varian HA-100 nmr spectrometer which was purchased with partial support of the NSF under Grant No. GP-5210. Partial support of this project by the University of Wisconsin Graduate Research Committee and the NSF under Grant No. GP-4566 is also gratefully acknowledged.

## Appendix I

**Detailed Solution of the Line-Shape Equations.** Equation 6 of the text gives the line shape as  $I(\omega) \propto \sum_A \text{Im } z_A$ , where the  $z_A$ 's are given by eq 7 in the form

$$(\mathbf{S} - \mathbf{I}\omega)\mathbf{z} = -\mathbf{a} \quad (\text{I-1})$$

To obtain the line shape, the eigenvalue problem for  $\mathbf{S}^T$  ( $\mathbf{S}$ -transpose) is first solved.

$$\mathbf{S}^T \mathbf{e}^i = \lambda_i \mathbf{e}^i \quad (\text{I-2})$$

Taking the inner product of  $\mathbf{e}^i$  with the transpose of eq I-1 gives

$$\mathbf{z}^T (\mathbf{S}^T - \mathbf{I}\omega) \mathbf{e}^i = \mathbf{z}^T (\lambda_i - \omega) \mathbf{e}^i = -\mathbf{a}^T \cdot \mathbf{e}^i$$

or

$$(\mathbf{e}^i)^T \cdot \mathbf{z} = -(\mathbf{e}^i)^T \cdot \mathbf{a}$$

Repeating this for each eigenvector, eq I-2 may be written as the single equation

$$\mathbf{e}\mathbf{z} = \mathbf{r} \quad (\text{I-3})$$

where  $[e]_{ij} = e_j^i = j$ th element of the  $i$ th eigenvector,  $r_i = d_i/(\lambda_i + \omega)$ , and  $d_i = -\mathbf{e}^i \cdot \mathbf{a}$ . Now defining  $\mathbf{e} = \mathbf{f} + i\mathbf{g}$ ,  $W_i = \text{Re}[r_i/(\lambda_i + \omega)]$ ,  $Y_i = \text{Im}[r_i/(\lambda_i + \omega)]$ , and  $\mathbf{z} = \mathbf{u} + i\mathbf{v}$ , the real and imaginary parts of eq I-3 can be separated and the solution becomes

$$\text{Im } \mathbf{z} = \mathbf{V} = (\mathbf{g}\mathbf{f}^{-1}\mathbf{g} + \mathbf{f})^{-1}(\mathbf{Y} - \mathbf{g}\mathbf{f}^{-1}\mathbf{W})$$

with

$$I(\omega) = \sum_i V_i$$

All calculations were done on the Control Data Corporation 1604 computer available at the University of Wisconsin Computing Center (UWCC). The line-shape equations were solved by our own subroutine, SYMLINE, using the procedure outlined above. Within SYMLINE the complex eigenvalue problem was solved with the UWCC library subroutine CMLXIEIG, which first reduces the matrix to upper Hessenberg form by a series of similarity transformations and then applies the QR transformation to this upper Hessenberg matrix.<sup>14</sup> In CMLXIEIG, convergence is accelerated by origin shifting and the eigenvectors are obtained by inverse iteration. Inversion of real matrices was done by the method of triangular decomposition, with iterative improvement, using the UWCC library routine MXINV.

The subroutine SYMLINE, adapted to be run as an independent program and renamed SYMSPEC, was used to compute spectra from given sets of parameters. Results were obtained in both tabular form and as plots from the CalComp plotter.

(14) See, for example, J. H. Wilkinson, "The Algebraic Eigenvalue Problem," Oxford University Press, London, 1965.

The least-squares fits of our model to the experimental spectra were accomplished by the UWCC library GAUSHAUS, which uses an iterative technique due to Marquardt.<sup>15</sup> This technique employs a combination of the Gauss (Taylor series) method and the method of steepest descent.

## Appendix II

### Reducing the Dimension of the Relaxation Matrix.

Consider a spin system with  $N$  allowed transitions, the first  $n$  of which are degenerate. We wish to find the conditions under which the degenerate transitions can be treated as a single transition, that is, the conditions under which the  $n$  equations in  $z_B$ ,  $1 < B < n$ , may be replaced by a single equation in the new variable  $Z$ , where  $Z = \sum_{B=1}^n z_B$ . To do this we sum eq 5 over the degenerate transitions

$$i\Delta Z + \sum_{B=1}^n \left( \sum_{A=1}^n R_{AB} \right) z_B = -ia \quad (\text{II-1})$$

where  $\Delta = \omega - \omega_A$  (a constant for all  $A$ ,  $1 < A < n$ ) and  $a = \sum_{A=1}^n a_A$ . To complete this reduction it is necessary that the sum in eq II-1 be rewritten

$$\left( \sum_{A=1}^n R_{AB} \right) \sum_{B=1}^n z_B + \sum_{B=n+1}^n \left( \sum_{A=1}^n R_{AB} \right) z_B$$

Thus we must have

$$\sum_{A=1}^n R_{AB} = \text{constant for all } B \quad 1 < B < n \quad (\text{II-2})$$

Similarly, if  $M$  is one of the nondegenerate transitions, we must also have

$$R_{MB} = \text{constant for all } B \quad 1 < B < n \quad (\text{II-3})$$

These conditions are easily generalized to cases with sev-

	$a\phi_A \rightarrow b\phi_A$	$b\phi_A \rightarrow c\phi_A$	$c\phi_A \rightarrow d\phi_A$	$a\phi_B \rightarrow b\phi_B$	$b\phi_B \rightarrow c\phi_B$	$c\phi_B \rightarrow d\phi_B$	
$a\phi_A \rightarrow b\phi_A$	$-54J^0 + \sum c_r$	0	$18J^0$	...	$c_B$	0	0
$b\phi_A \rightarrow c\phi_A$	0	$-36J^0 - \sum c_r$	0	...	0	$c_B$	0
$c\phi_A \rightarrow d\phi_A$	$18J^0$	0	$-54J^0 - \sum c_r$	...	0	0	$c_B$

(II-4)

eral sets of degenerate transitions.

(15) D. L. Marquardt, *J. Soc. Ind. Appl. Math.*, 2, 431 (1963).

The elements of the relaxation matrix are given explicitly by eq 8 and 9 of the text. We shall now assume that the spin operators,  $A^q$ , appearing in these equations are of two types: ones which operate only on boron spins, such as the quadrupole operator, and those which operate only on hydrogen spins, such as the chemical exchange operator of our problem. Taking the quadrupole operators from Abragam,<sup>4</sup> we calculate the two typical blocks of the  $R$  matrix (II-4). The hydrogen spin functions are denoted by  $\phi_A$  and  $\phi_B$ , and  $a, b, c$ , and  $d$  represent boron spins of  $3/2, 1/2, -1/2$ , and  $-3/2$ , respectively.

The  $c$ 's represent the effects of pure hydrogen operators, and the sum appearing in each diagonal element is the sum of the  $c$ 's appearing in the off-diagonal positions of that same row (see eq 12). In case  $\phi_A$  and  $\phi_B$  are related by spin exchange, as described in the text,  $c$  would be the frequency of that exchange. If hydrogen-hydrogen dipole relaxation were included, the transition probabilities for these processes would be added into the  $c$ 's as well. It is hydrogen relaxation mechanisms such as these that the two parameters  $Q_1$  and  $Q_2$ , which proved unimportant in our case, would represent.

Summing up each column of the diagonal block gives the result  $-36J^0 - \sum c_r$ , and summing each column of the off-diagonal block gives  $c_B$ . Thus conditions II-2 and II-3 are satisfied, as we wanted to show. It should be noted that these conditions are not met in the presence of boron-hydrogen cross-relaxation *via* the dipole-dipole interaction, as a quick calculation of a few elements will show. Our assumption that these are unimportant is borne out by our success in fitting the experi-

mental spectra and is due to the predominance of quadrupole relaxation in  $^{11}\text{B}$  relaxation.